

The effect of the Madden-Julian Oscillation on station rainfall and river level in the Fly River system, Papua New Guinea

Adrian J. Matthews,^{1,2} Geoff Pickup,³ Simon C. Peatman,² Peter Clews,⁴ and Jason Martin⁴

Received 18 April 2013; revised 26 September 2013; accepted 26 September 2013; published 10 October 2013.

[1] The Madden-Julian oscillation (MJO) is the dominant mode of intraseasonal variability in tropical rainfall on the large scale, but its signal is often obscured in individual station data, where effects are most directly felt at the local level. The Fly River system, Papua New Guinea, is one of the wettest regions on Earth and is at the heart of the MJO envelope. A 16 year time series of daily precipitation at 15 stations along the river system exhibits strong MJO modulation in rainfall. At each station, the difference in rainfall rate between active and suppressed MJO conditions is typically 40% of the station mean. The spread of rainfall between individual MJO events was small enough such that the rainfall distributions between wet and dry phases of the MJO were clearly separated at the catchment level. This implies that successful prediction of the large-scale MJO envelope will have a practical use for forecasting local rainfall. In the steep topography of the New Guinea Highlands, the mean and MJO signal in station precipitation is twice that in the satellite Tropical Rainfall Measuring Mission 3B42HQ product, emphasizing the need for ground-truthing satellite-based precipitation measurements. A clear MJO signal is also present in the river level, which peaks simultaneously with MJO precipitation input in its upper reaches but lags the precipitation by approximately 18 days on the flood plains.

Citation: Matthews, A. J., G. Pickup, S. C. Peatman, P. Clews, and J. Martin (2013), The effect of the Madden-Julian Oscillation on station rainfall and river level in the Fly River system, Papua New Guinea, *J. Geophys. Res. Atmos.*, 118, 10,926–10,935, doi:10.1002/jgrd.50865.

1. Introduction

[2] The Madden-Julian Oscillation (MJO) is a planetary-scale, long-lived weather system. It primarily consists of a large-scale ($\sim 10,000$ km) region of enhanced precipitation that originates over the tropical Indian Ocean then propagates slowly eastward over the maritime continent to the western Pacific. These precipitation anomalies are accompanied by coherent global-scale dynamical patterns in wind, pressure, and temperature. A single MJO event or cycle typically lasts 30–60 days. Although there is not yet a complete theory of the MJO and many models have considerable difficulties in simulating it, skillful operational forecasts of the MJO are now routinely made out to lead times of up to a few weeks [Jones *et al.*, 2004; Wheeler and Hendon, 2004; Waliser, 2005; Love *et al.*, 2008; Love and Matthews, 2009].

[3] These forecasts all predict the evolution of only the largest-scale MJO features. However, the large-scale MJO envelope of precipitation is itself comprised of many smaller mesoscale weather systems [Nakazawa, 1988], which themselves have many embedded individual cumulonimbus elements (~ 10 km scale). Scale interaction is at the heart of the MJO. In one paradigm, the large-scale conditions in the MJO provide the environment in which small-scale convection develops. The small-scale systems then self-organize through mesoscale processes, and their spatially aggregated fluxes and latent heat release feed back onto the large-scale circulation. For a comprehensive review of the MJO, see Zhang [2005].

[4] The large-scale MJO envelope is very clear when it is analyzed in global-gridded precipitation data sets [Sperber, 2003; Waliser *et al.*, 2009]. However, as smaller scales are examined, the stochastic nature of precipitation becomes more important, and the large-scale signal can be obscured. This effect is felt most strongly at the meteorological station level, where a rain gauge effectively makes a point measurement of precipitation. An individual cumulonimbus element embedded in the large-scale MJO envelope may by chance pass directly over the rain gauge, which would record a significant amount of precipitation. Alternatively, the cumulonimbus may by chance pass several kilometers to the side, with little or no precipitation being recorded at the rain gauge.

¹Centre for Ocean and Atmospheric Sciences, School of Environmental Sciences, University of East Anglia, Norwich, UK.

²Centre for Ocean and Atmospheric Sciences, School of Mathematics, University of East Anglia, Norwich, UK.

³Consulting Geomorphologist, Sutton, New South Wales, Australia.

⁴Ok Tedi Mining Limited, Tabubil, Papua New Guinea.

Corresponding author: A. J. Matthews, School of Environmental Sciences, University of East Anglia, Norwich, NR4 7TJ, UK. (a.j.matthews@uea.ac.uk)

©2013. American Geophysical Union. All Rights Reserved.
2169-897X/13/10.1002/jgrd.50865

[5] The societal effects of precipitation are often felt at these very small, local scales. For example, small-scale rain-fed agriculture or local industrial operations may be crucially dependent on the precipitation in the immediate vicinity but care little about large-scale aggregated rainfall patterns. Hence, the question of whether a large-scale system such as the MJO is “felt” at the local level can be an important one.

[6] Surprisingly, there have been relatively few studies of the MJO at the individual station level. Even where the large-scale MJO envelope of precipitation is strong, such as over the western Pacific, the local signal may be difficult to detect at the rain gauge scale. For example, *Matthews and Li* [2005] analyzed daily rainfall data from 140 individual stations on islands in the western Pacific. The sign of the rainfall anomaly at 80% of the stations during each of four phases of the MJO was consistent with the sign of the large-scale MJO rainfall pattern in the Climate Prediction Center Merged Analysis of Precipitation data set [*Xie and Arkin*, 1997]. However, to obtain statistically significant rainfall anomalies, the individual station data had to be spatially aggregated into $10 \times 10^\circ$ boxes then temporally aggregated into a crude “wet” minus “dry” MJO field before a convincing signal could be found.

[7] Gridded station rainfall has been shown to exhibit clear MJO signals in other regions, such as India [*Hartmann and Michelsen*, 1989; *Krishnamurthy and Shukla*, 2000], East Africa [*Mutai and Ward*, 2000], and the western United States [*Bond and Vecchi*, 2003]. However, only a few studies have revealed a strong MJO signal at the individual station level. These include China [*Zhang et al.*, 2009], Afghanistan [*Barlow et al.*, 2005], Southeast Asia, and the maritime continent [*Donald et al.*, 2006].

[8] The maritime continent comprises the archipelago of the islands of several countries, including Indonesia, Malaysia, Papua New Guinea, and their surrounding seas. It lies at the heart of the tropical warm pool and experiences some of the highest rainfall totals on the planet. The large-scale latent heat release associated with this precipitation triggers planetary Rossby waves and thereby a strong controlling influence on global circulation and climate.

[9] In particular, the maritime continent lies in the center of the path of the MJO and has a very strong MJO precipitation signal when diagnosed from large-scale precipitation data sets [*Sperber*, 2003]. *Donald et al.* [2006] and *Kanamori et al.* [2013] also presented evidence of the effect of the MJO on precipitation over the maritime continent at the station level, but detailed results at the individual station level have not been shown.

[10] The Ok Tedi mine is located in the highlands of Papua New Guinea at the head of the Fly River system [*Bolton*, 2009] at approximately 141°E , 5°S . It is a major world producer of copper and gold and has been operational since the mid-1980s. Transportation of materials by boat along the Fly River system, between the mine and the coast, is susceptible to extreme precipitation and subsequent changes in river level and flow. Hence, to facilitate mining operations, a series of meteorological and hydrological stations has been established along this route. The continuous long-term data sets from these stations provide an unprecedented source of high-quality geophysical information from this remote region.

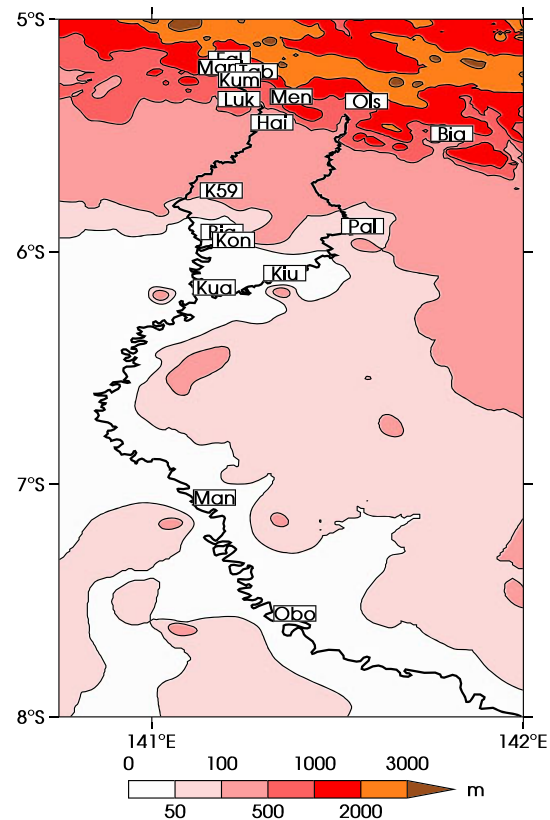


Figure 1. Map of station locations and orographic height (m; see legend for shading levels). The station locations are at the southwestern corner of the labeled boxes. Further station details are given in Table 1. The Ok Tedi and Fly rivers are shown by the thick black lines.

[11] In this paper, the MJO signal at the individual station level is presented for the first time in such detail for a location in the maritime continent, the core region of MJO activity. The MJO effect on river level is also presented for the first time for any location. MJO signals are strong at nearly all stations, and the implications for local agriculture and industry are discussed.

2. Data

[12] The primary data used in this study are the time series of daily rainfall totals from rain gauges at 15 meteorological stations along the Fly River system in Papua New Guinea (Figure 1). The stations have been grouped into four main river catchments: Upper Ok Tedi and Upper Fly are in the mountainous highlands; Lower Ok Tedi and Middle Fly are in the low-lying flood plains (Table 1). The orography used in Figure 1 is the Globe Land One-kilometer Base Elevation (GLOBE) data set [*Hastings et al.*, 1999], regridded to 0.11° resolution.

[13] Some stations (e.g., Tabubil, next to the mine) have been operational since the preliminary activities commenced in the early 1970s, but most were established later (Figure 2). The 16 year period from 1992 to 2008 was used as a compromise to maximize both the length of the study period and the number of operational rain gauges.

Table 1. Station Details^a

River Catchment	Station Name	Code	Precip.	Hydro.	Location	$N(\%)$	N_h
Upper Ok Tedi	Falomian	Fal	○		141.15°E, 5.20°S	2900 (100%)	
Upper Ok Tedi	Ok Mani	Mani	□		141.12°E, 5.24°S	2514 (87%)	
Upper Ok Tedi	Tabubil	Tab	×		141.22°E, 5.26°S	2900 (100%)	
Upper Ok Tedi	Kumkit	Kum	+		141.18°E, 5.29°S	2766 (95%)	
Upper Ok Tedi	Ok Menga	Men	*		141.31°E, 5.37°S	2554 (88%)	
Upper Ok Tedi	Haidauwogam	Hai	◇		141.26°E, 5.48°S	2783 (96%)	
Upper Ok Tedi	Lukwi	Luk		▽	141.17°E, 5.38°S		23
Upper Fly	Olsobip	Ols	○		141.52°E, 5.39°S	2840 (98%)	
Upper Fly	Biangabip	Bia	□		141.75°E, 5.53°S	2767 (95%)	
Upper Fly	Kiunga	Kiu	×		141.30°E, 6.12°S	2820 (97%)	
Upper Fly	Palmer R Junction	Pal		+	141.51°E, 5.92°S		10
Lower Ok Tedi	Pump Stn Km59	K59	○		141.13°E, 5.77°S	2494 (86%)	
Lower Ok Tedi	Bige	Big	□		141.13°E, 5.95°S	1985 (68%)	
Lower Ok Tedi	Konkonda	Kon	×	×	141.16°E, 5.98°S	2659 (92%)	27
Middle Fly	Kuambit	Kua	○	○	141.11°E, 6.19°S	1053 (36%)	20
Middle Fly	Manda Village	Man	×	×	141.11°E, 7.09°S	1088 (38%)	17
Middle Fly	Obo	Obo	+	+	141.32°E, 7.59°S	2189 (75%)	23

^aCode refers to the station code on the map in Figure 1. The precip. and hydro. columns indicate whether a station is a precipitation or hydrological (river level) station, or both; the symbols are used on the line diagrams for the corresponding station in Figure 5. N is the number of days of data in November–April 1992–1993 to 2007–2008 (in brackets as a percentage of total) for the precipitation stations. N_h is the number of years (November–April seasons) of river level data for the hydrological stations.

[14] Large-scale rainfall patterns were analyzed using the Tropical Rainfall Measuring Mission (TRMM) 3B42HQ “high-quality” precipitation product [Huffman *et al.*, 2007] that only uses direct measurement of precipitation by satellite-based microwave sensors. The analysis was also carried out with the merged (microwave and infrared) 3B42 product; results were very similar. The data were available as 3-hourly maps on a $0.25^\circ \times 0.25^\circ$ grid. The TRMM data began in 1998. As the optimal period of station data coverage ends in 2008, only TRMM data from 1998–2008 were used.

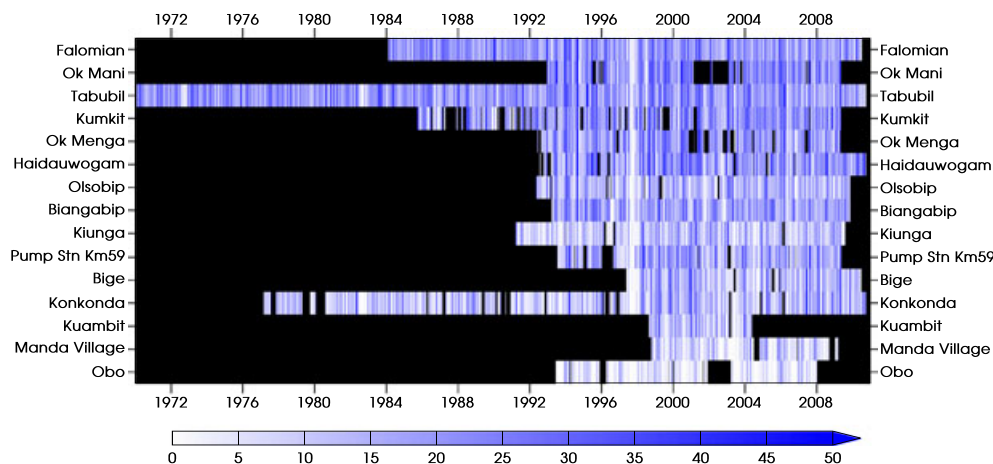
[15] During northern winter (November–April), New Guinea is at the heart of the mean monsoon rainfall envelope over the tropical warm pool (Figure 3a). The Fly River study region (same domain as the map in Figure 1) is shown by the small box over central New Guinea in the left panels of Figure 3. The mean rainfall in the Fly River domain is then expanded in the right panels of Figure 3. During northern winter, the mean rainfall over the Fly River domain is consistently high, from 10 mm d^{-1} over the low-lying southern

flood plains to over 16 mm d^{-1} in the north on the flanks of the mountains.

[16] However, during northern summer (May–October), the monsoon has migrated northward, and New Guinea lies on the southern flank of the mean rainfall envelope (Figure 3b). Although there is still significant rainfall over the Fly River domain, it is much weaker, varying from below 4 mm d^{-1} in the south to 12 mm d^{-1} in the north.

[17] The MJO also changes characteristics between these two seasons, broadly following the envelope of mean monsoon rainfall. During northern winter, the MJO exhibits its canonical behavior of eastward propagation, with New Guinea at the heart of its envelope [e.g., Wheeler and Hendon, 2004]. During northern summer, the MJO also develops a northward-propagating component and is strongest over the Southeast Asian mainland to the north. The Fly River domain is right at the edge of the MJO influence during this season.

[18] Hence, the analysis of the MJO signal in the station rainfall, presented here, is for the northern winter

**Figure 2.** Daily rainfall totals for each station (mm d^{-1}). Black areas indicate no coverage.

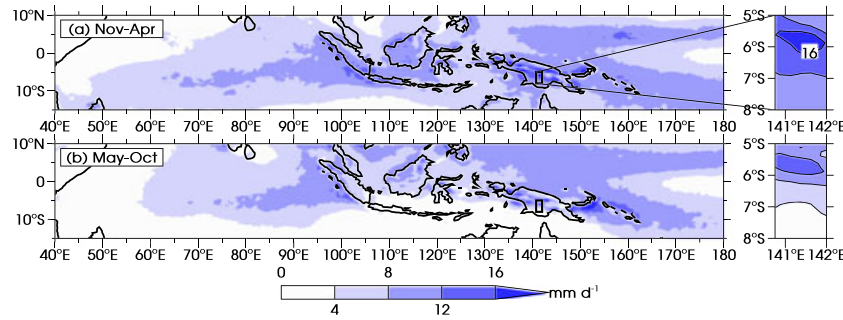


Figure 3. Mean TRMM precipitation for (a) November–April and (b) May–October. The box over central New Guinea in the left panels is the domain of the map in Figure 1. The right panels show a blowup of this domain. Contour interval is 4 mm d^{−1}. See legend for shading intervals.

(November–April) season only. When the analysis was repeated with all-year-round data, the results were similar to those for northern winter, but the MJO effect on the station rainfall was not quite as clearly defined.

[19] Two study periods were defined. The main period was defined by the 16 November–April seasons from 1992–1993 to 2007–2008, a total of 2900 days. The number of days (total and as a percentage of total) of operation for each station in this period is shown in the final column in Table 1. Falomian and Tabubil stations have 100% coverage. There are 11 stations with greater than 85% coverage. A subset of this period (10 November–April seasons from 1998–1999 to 2007–2008) was also used to allow a direct comparison between station rainfall data and TRMM data.

3. MJO Envelope

[20] The Realtime Multivariate MJO (RMM) index of *Wheeler and Hendon* [2004] was used to define and diagnose the MJO. The indices were available as daily time series. The RMM indices were used to construct composite maps of the large-scale TRMM 3B42HQ precipitation anomalies throughout the MJO cycle. To calculate the anomalies, the 3-hourly data were averaged to daily means then an annual cycle (time mean and first six annual harmonics) was removed to produce anomaly maps.

[21] Following *Wheeler and Hendon* [2004], the MJO is conveniently divided into eight phases, each of which typically lasts 6 days ($8 \times 6 = 48$ days, a typical lifetime of an MJO event). The RMM index can be expressed as a daily value of an amplitude (normalized to have a standard deviation of 1) and a phase (an integer from 1 to 8). For a given phase, the days when the RMM index is in that phase, and its amplitude greater than 1, are selected. During November–April 1998–2008, this produces between 28 (phase 1) and 41 (phase 4) blocks of time, of typical length 3–8 days. For example, there are 28 blocks for MJO phase 1 (13–17 January 1999, 26–28 February 1999, ..., 2–9 March 2008, 10–11 April 2008). The TRMM precipitation maps on these days are averaged to produce a composite map for that MJO phase.

[22] The composite map for MJO phase 1 (Figure 4a) shows a region of positive precipitation anomalies (active, enhanced convection, wetter than usual) over the central Indian Ocean. There are also negative precipitation anomalies (suppressed convection, drier than usual) over the mari-

time continent sector. This “dipole” pattern is a well-known feature of the MJO. However, even though the MJO envelope is one of suppressed, dry conditions over the maritime continent sector, within this there are enhanced, wet conditions over some of the islands (Sumatra, Borneo, and western New Guinea). This “vanguard” of convection over the islands has been recently identified and interpreted as a triggering of the diurnal cycle ahead of the main MJO envelope [Peatman *et al.*, 2014]. The Fly River system study area is shown by the small box in central New Guinea in Figure 4a; this corresponds to the domain of the map in Figure 1. This domain is expanded in the right panel of Figure 4a. The MJO signal in this region mainly has slightly enhanced precipitation during MJO phase 1.

[23] The remaining seven phases of the MJO are shown in Figures 4b–4h. The progression of the MJO can be clearly seen, as its main active region moves slowly eastward across the maritime continent by phase 3 (Figure 4c) and into the western Pacific in phases 5 and 7 (Figures 4e and 4g).

[24] The peak precipitation over the Fly River area and most of New Guinea is in MJO phase 3 (Figure 4c), even though precipitation is still suppressed over the sea to the north and south of the island. The latter half of the MJO cycle (phases 5–8) shows an approximate reversal of the first half, with suppressed convection over the land of central New Guinea in phases 5 and 6 (Figures 4e and 4f) even though the surrounding ocean is still under active conditions. In phases 7 and 8 (Figures 4g and 4h) there is suppressed convection over both the land of New Guinea and the surrounding ocean.

4. MJO Cycle in Station Precipitation

4.1. Mean MJO Cycle

[25] The envelope of MJO precipitation over the Fly River system has been calculated from the TRMM precipitation (Figure 4). We now examine whether this large-scale signal is manifested at the individual station level, and if so, if it is consistent with the satellite-measured TRMM data. The composite MJO precipitation signal at each station is calculated using the same technique as for the TRMM composites. Only data during November–April 1998–2008 were used in the calculations here to allow a direct comparison with the TRMM data.

[26] The Upper Ok Tedi river catchment is located in the mountain highlands of central New Guinea (Figure 1).

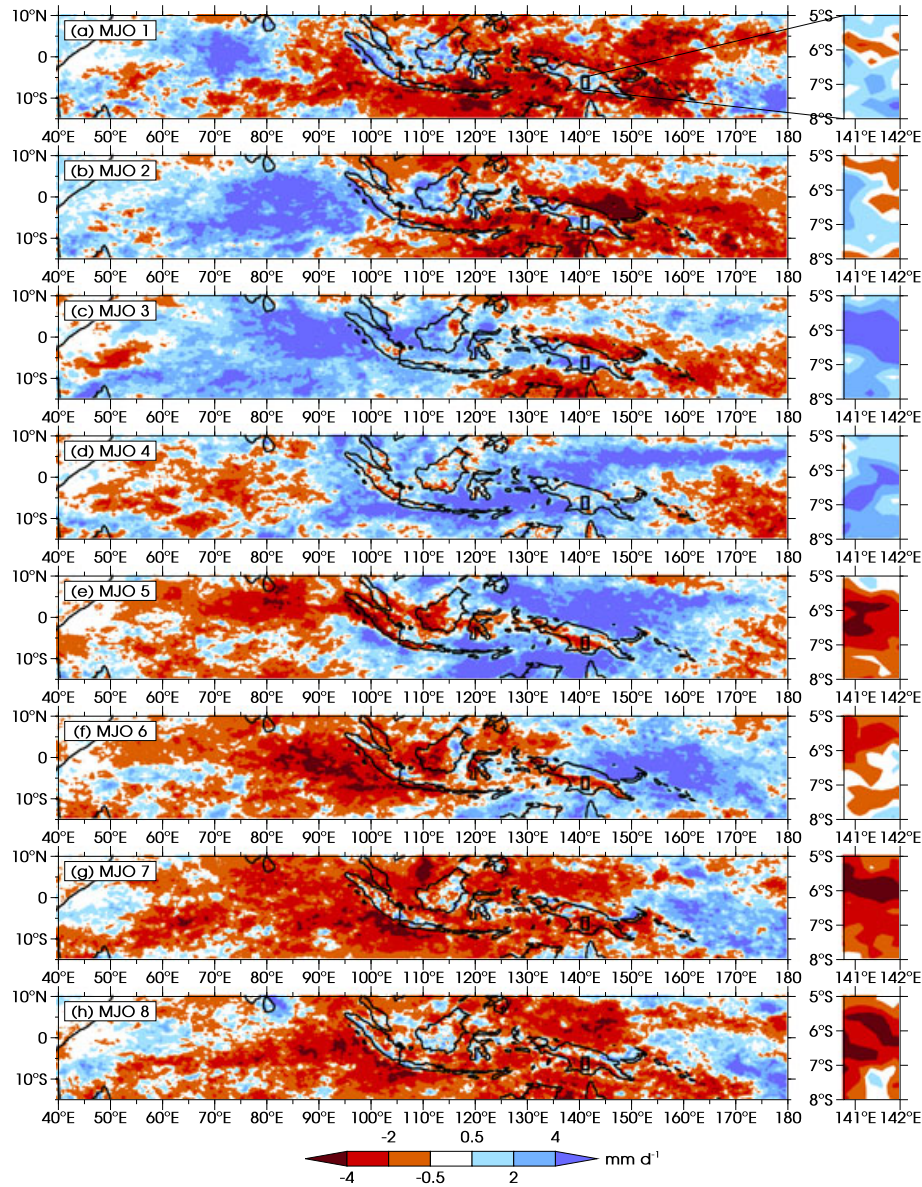


Figure 4. TRMM precipitation anomalies (mm d^{-1}) for MJO phases (a) 1, (b) 2, (c) 3, (d) 4, (e) 5, (f) 6, (g) 7, and (h) 8 during November–April 1998–2008. The box over central New Guinea in the left panels is the domain of the map in Figure 1. The right panels show a blowup of this domain. See legend for shading intervals.

The signal for each of the six meteorological stations in the Upper Ok Tedi are shown by the thin black solid lines in Figure 5a. These values are totals, not anomalies. The mean rainfall at these mountain stations is very high, at 23 mm d^{-1} .

[27] Statistical significance is assessed based on a Monte Carlo resampling technique. For a given Monte Carlo simulation, the time blocks used to create the original composite are randomized. First, the start time of a block is reset to a randomly chosen day within a ± 15 day window of the original start time. Then the year of the start time is randomized, within the 1998–2008 domain. The length of the original block is preserved. Hence, this resampling methodology preserves the autocorrelations and seasonal dependence in the original data. This randomization is carried out for each time block, and a composite mean station precipitation value is

calculated based on these randomized time blocks. This process is repeated 1000 times, and a null distribution built up from the 1000 randomized composite station precipitation values. The tails of this null distribution are then used to set the statistical significance thresholds. If the rainfall at a particular station is statistically significantly different from the mean at the 95% level (two-tailed test) during a particular MJO phase (for example, Ok Mani in MJO phases 4 and 7), then a second, oversized copy of the relevant symbol from Table 1 (a square for Ok Mani) is plotted on top of the line in Figure 5.

[28] Each individual station in the Upper Ok Tedi catchment shows a clear, smoothly varying signal throughout the MJO cycle, with very little noise, with a maximum in MJO phase 4, during the active stage of the MJO over New Guinea

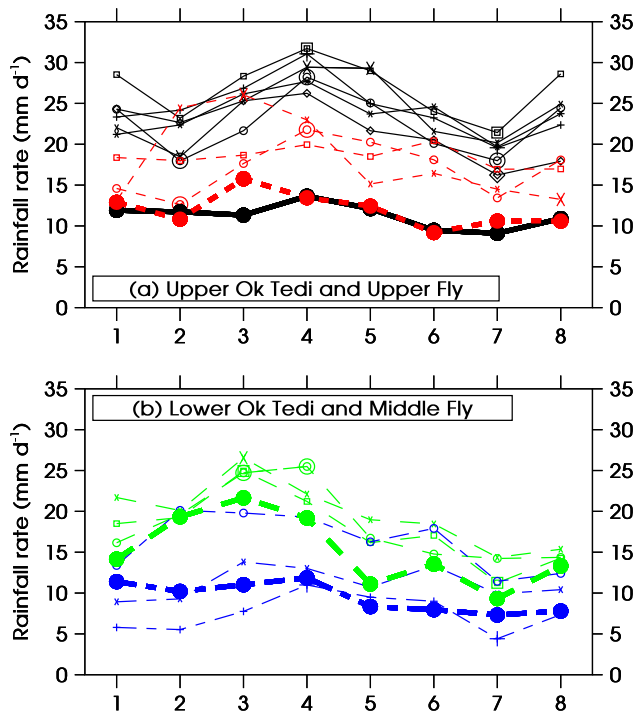


Figure 5. MJO cycle of rainfall rate (mm d^{-1}) at precipitation stations during November–April 1998–2008: (a) Upper Ok Tedi catchment (black solid lines) and Upper Fly catchment (red dotted lines); (b) Lower Ok Tedi catchment (green dashed lines) and Middle Fly catchment (blue dash-dotted lines). The symbols for each station correspond to those in Table 1. Where a particular data point is statistically significant at the 95% level, a second, oversized symbol is plotted. TRMM data at selected grid points are shown by the thick lines (see main text for details).

(Figure 5a). This maximum is statistically significant at five out of the six stations. Hence, the enhanced rainfall during phase 4 of the MJO clearly stands out above the background variability. Similarly, there is a minimum in precipitation at all stations, between MJO phases 7 and 2, during the suppressed half of the MJO cycle over New Guinea. Again, these minima are statistically significant at five out of six of the stations. A typical peak to trough difference is 9 mm d^{-1} , about 40% of the mean. Hence, the MJO has a very large effect on daily rainfall totals at the individual station level. Note that the actual totals recorded at each station will be strongly dependent on the details of the exposure of the rain gauge and local micrometeorological conditions. Hence, it is probably not meaningful to analyze the differences between the stations within the same catchment.

[29] The MJO signal in TRMM at the nearest grid point (141.125°E , 5.125°S) to these stations (thick black solid line in Figure 5a) shows a much weaker average value of 11 mm d^{-1} , about half that recorded at the individual stations. The MJO modulation is also much weaker with a peak to trough of only 5 mm d^{-1} . However, this is a similar 40% of the average as with the station data. The maximum precipitation at the TRMM grid point is at MJO phase 4, in agreement with the station data, although the TRMM maximum is broader and less well defined.

[30] Two out of the three meteorological stations in the Upper Fly catchment (Olsobip and Kiunga) also all show a clear MJO signal (thin red dotted lines in Figure 5a) with a peak in MJO phase 3 or 4. However, their mean and peak to trough values are reduced, compared to the stations in the Upper Ok Tedi. The TRMM precipitation at the nearest grid point (141.625°E , 5.325°S ; thick red dotted line in Figure 5a) also shows a much reduced mean and MJO variation compared with the station data. Here the TRMM precipitation peaks in MJO phase 3.

[31] The Lower Ok Tedi stations are in the more gently sloping foothills (Figure 1; it should be noted that Kiunga on the Upper Fly is also in these foothills). The rainfall at the three stations here (thin green dashed lines in Figure 5b) peaks in MJO phase 3 or 4. The TRMM rainfall from the nearest grid point (141.125°E , 5.875°S ; thick green dashed line in Figure 5b) agrees fairly closely with the station data, although it has consistently slightly lower values, with a maximum of 22 mm d^{-1} in MJO phase 3 and a minimum of 9 mm d^{-1} in phase 7.

[32] Further downstream, the Middle Fly river catchment is on the flat flood plains (Figure 1). Kuambit, the first station on the Middle Fly is geographically very close to the stations just upstream and also has a strong MJO signal with a broad precipitation maximum in MJO phases 2–4 and a minimum in phase 7 (thin blue dash-dotted line with circles in Figure 5b).

[33] Manda Village and Obo are much further downstream (100–150 km to the south) on the flood plains well away from the mountains. Without any orographic enhancement, the mean precipitation here is much less and hence the absolute magnitude of the MJO signal at these two stations is correspondingly smaller. However, it is still significant at Obo; the rainfall in the wet MJO phase 4 (11 mm d^{-1}) and dry MJO phase 7 (4 mm d^{-1}) are both statistically significantly different from the mean rainfall (7 mm d^{-1}) at the 95% level. This peak to peak difference represents a 100% modulation of the mean rainfall.

[34] It may at first seem surprising that the MJO signal varies so much over the relatively small scale of the Fly River study area (approximately 200 km between the most northern and southern stations), compared to the much larger scale of the MJO convective envelope (several thousand kilometers, Figure 4). However, the MJO exhibits a strong multiscale structure [Nakazawa, 1988]. Precipitation falling from the MJO superclusters will have variability on much smaller scales due to internal convective and mesoscale dynamics and interaction with the underlying high, steep, and rapidly varying topography.

4.2. Variability Between MJO Events

[35] In section 4.1 the average rainfall was calculated as the straightforward mean over all days when the RMM index was in a particular MJO phase. For example, there were 141 days in MJO phase 4 during the November–April 1998–2008 period. While this was effective in establishing that there were significant changes in mean station rainfall during some phases of the MJO, it gave no information on the spread of rainfall between MJO events.

[36] Care needs to be taken in calculating this spread. The day-to-day variability at an individual station is very large; recorded rainfall can be zero one day and over 100 mm the

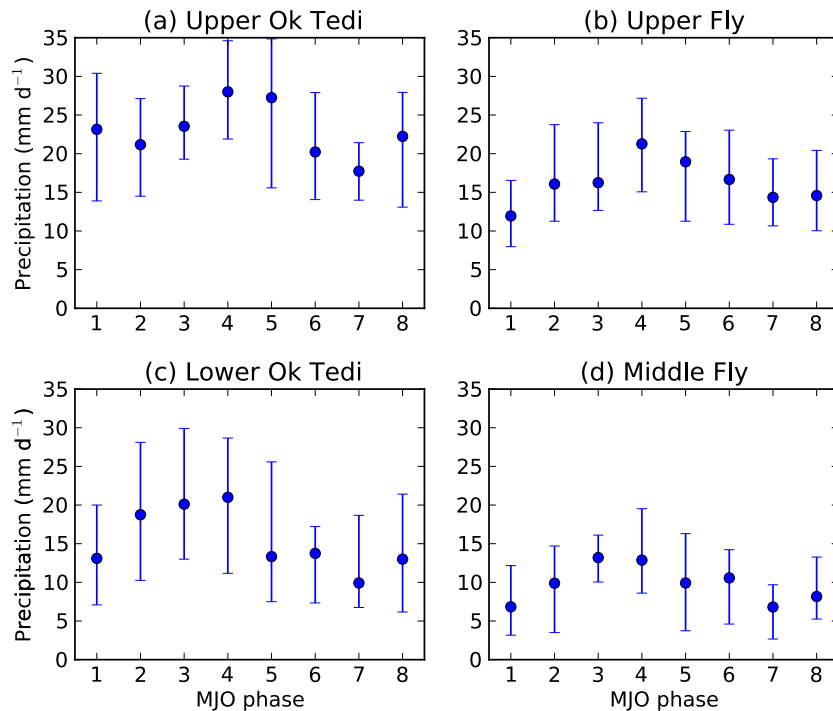


Figure 6. MJO cycle of rainfall rate (mm d^{-1}) aggregated to catchment scale during November–April 1992–2008: (a) Upper Ok Tedi, (b) Upper Fly, (c) Lower Ok Tedi, and (d) Middle Fly. The circles show the median of the event mean rainfall distribution, and the error bars show the interquartile range of the distribution.

next day. Hence, any measure of spread based on raw daily values will be dominated by this variability, and no MJO signal will emerge. As the MJO is a slowly varying phenomenon, with a time scale measured in weeks, it would not make physical sense to analyze the spread in the daily data anyway. Hence, some time averaging is necessary, and event means are first calculated. For example, the 141 days that were in MJO phase 4 during November–April 1998–2008 were comprised of 41 separate blocks of days, each block, or “event,” corresponding to the phase 4 of an individual MJO. Each event typically lasts 3–6 days. The mean rainfall was calculated for each event, leading to a population of, in this case, 41 event means for MJO phase 4 at each station. In practice, the size of the population would be somewhat less than 41 here, due to missing data, and an additional condition wherein only events that lasted at least 2 days were included.

[37] Further averaging was then carried out by spatially averaging over all stations within the same catchment (Table 1). Again, because of missing data, a minimum coverage was stipulated so that an event and catchment mean value were only included if at least two stations in the catchment contributed to that data point.

[38] Hence, for each MJO phase and catchment, a distribution of event mean rainfall rates was produced. The median and interquartile range of each of these distributions are shown in Figure 6. To test the robustness of the results further, the full station data set for November–April 1992–2008 was used. Results for the November–April 1998–2008 TRMM-overlapping data set were very similar.

[39] The median of the event mean rainfall distribution during MJO phase 4 in the Upper Ok Tedi catchment dur-

ing November–April 1992–2008 was 28 mm d^{-1} (Figure 6a). This is clearly consistent with the unweighted mean rainfall values at the individual stations in the Upper Ok Tedi (black lines in Figure 5a, in the range $26\text{--}32 \text{ mm d}^{-1}$ during MJO phase 4) during the shorter period of November–April 1998–2008. This general consistency is evident at all MJO phases, in all catchments, confirming that the calculation of the MJO cycle of rainfall is robust and not sensitive to methodology or study period.

[40] The spread of rainfall between MJO events can be measured by the interquartile range, shown as the error bars in Figure 6. For MJO phase 4 (the wettest part of the MJO cycle) in the Upper Ok Tedi catchment, the interquartile range is from 22 to 35 mm d^{-1} (Figure 6a). In phase 7 (the driest part of the MJO cycle), the median rainfall is 18 mm d^{-1} , outside the interquartile range of (the wet) phase 4. There is also no overlap of the center halves of the two distributions, with the interquartile range in phase 7 at $14\text{--}22 \text{ mm d}^{-1}$. Hence, in addition to the mean rainfall being significantly different between the wet and dry phases, the probability distributions of the expected rainfall in these two MJO phases are also well separated. This is a significant result, as it implies useful predictability of rainfall at the local level for individual MJO events, if the large-scale evolution of the MJO can be forecasted.

[41] In the Upper Fly and Lower Ok Tedi catchments, although there is a clear MJO cycle, the distributions of rainfall in the wet and dry phases of the MJO are not quite as clearly separated (Figures 6b and 6c). However, in the Middle Fly catchment, there is again a distinct separation in the rainfall distributions between the wet phase (3) and the dry phase (7).

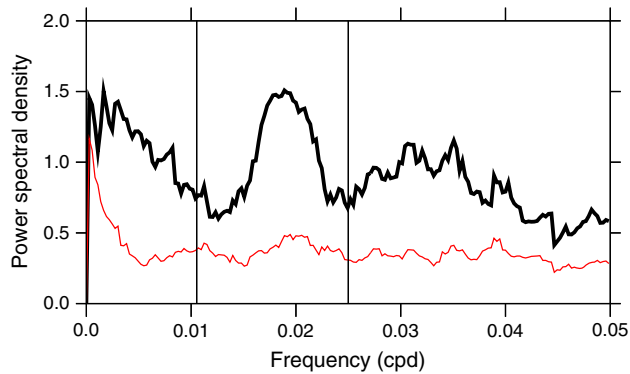


Figure 7. Smoothed power spectra of daily precipitation time series for the Upper Ok Tedi catchment: station data (thick line) and TRMM data (thin line). The vertical lines are at frequencies of 1/95 and 1/35 cpd, and correspond to the frequency band of the MJO.

4.3. Power Spectra

[42] Fourier analysis has been applied to the MJO many times; indeed, it was the technique used to discover the oscillation [Madden and Julian, 1971, 1972]. Power spectra of time series can be examined for spectral peaks in the frequency range of the phenomenon, approximately 1/95 to 1/35 cycles per day (cpd) for the MJO [Salby and Hendon, 1994]. However, Fourier techniques are problematic when dealing with precipitation time series, which tend not to vary smoothly, and have a fixed baseline minimum (zero). This problem is exacerbated by any missing data.

[43] Nevertheless, it is of interest to apply Fourier techniques to the station and TRMM precipitation time series to search for enhanced power at MJO frequencies. Missing data were set to zero. Individual station time series are very noisy, and no clear spectral peaks are evident in their spectra (not shown). The time series of the six stations in the Upper Ok Tedi catchment (Table 1) were then averaged together. The power spectrum was calculated from the 10 year time series of this catchment mean daily precipitation, starting from 1 January 1998. Following Wilks [2005], the spectrum was smoothed, using a 21 point running mean. The power spectrum does show a clear peak between frequencies of approximately 0.017–0.022 cpd (thick line in Figure 7). This corresponds to time periods in the 45–60 day range, within the MJO band.

[44] A corresponding TRMM precipitation time series for the Upper Ok Tedi catchment was calculated by averaging over the box from 141.0 to 141.5°E and from 5.0 to 5.5°S. The overall power in the TRMM power spectrum (thin line in Figure 7) is much lower than in the station data. This is consistent with the mean and (MJO) variability being at a lower amplitude, as discussed in section 4.1. Additionally, although there is a peak in the MJO frequency range, it does not stand out clearly from the remainder of the spectrum. Hence, for the Upper Ok Tedi catchment, the MJO precipitation signal is stronger, in terms of a spectral peak, in the station data than in the satellite TRMM data. Problems with the TRMM data are discussed in section 6.

[45] Catchment mean time series and power spectra of station data were calculated for the other three catchments:

Upper Fly, Lower Ok Tedi, and Middle Fly. Although there were peaks in the MJO frequency range, they did not stand out convincingly above the background. This is likely due to a combination of more missing data at these stations (Figure 2) and/or a genuinely weaker MJO signal (Figure 5) relative to the mean precipitation.

5. MJO Cycle in River Level

[46] Daily river level data were available at six hydrographical stations on the Fly River system. The lengths of these time series ranged from 10 to 27 years (Table 1). Composite MJO cycles of river level were calculated as for the station precipitation. Results are presented as anomalies from the mean river level at each station (Figure 8).

[47] All the stations show a clear, unambiguous MJO cycle in river level. The two stations in the mountainous highland region near the rivers' headwaters (Lukwi on the Upper Ok Tedi, black solid line; and Palmer Junction on the Upper Fly, red dotted line) both show peak water levels in MJO phase 4, up to 0.75 m above the mean level. This coincides with the peak in rainfall at these locations (Figure 5a). Hence, the river response to rainfall on these intraseasonal time scales is essentially instantaneous. Both these hydrological stations have minimum river level in MJO phase 7, up to 0.5 m below the mean, coinciding with the minimum in MJO station rainfall, again consistent with a very fast response of the river to the local rainfall.

[48] Moving downstream into the Lower Ok Tedi (Konkonda, green dash-dotted line) and Middle Fly (Kuambit, blue dashed line with circles) catchments, the maximum river level is now later in the MJO cycle, at phase 5. This is despite the local rainfall being a maximum in MJO phases 3–4 (Figure 5b). This delay is due to the integrated response to the rainfall further upstream. There is then an advective time delay for this signal to be transmitted downstream. Additionally, there are large off-river water bodies along the flood plains that fill when the river level is high, and drain with the river level drops. These act to further delay the downstream response to rainfall. The total time delay between rainfall input and river response at these

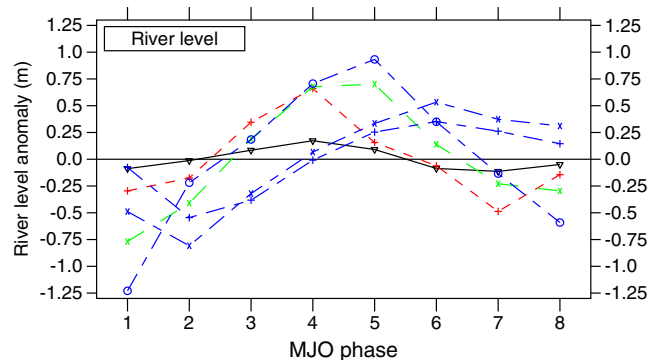


Figure 8. MJO cycle of river level anomaly (m) at river gauging stations: Upper Ok Tedi catchment (black solid line: Lukwi), Upper Fly catchment (red dotted line: Palmer), Lower Ok Tedi catchment (green dashed line: Konkonda), and Middle Fly catchment (blue dash-dotted lines: Kuambit (circles), Manda (cross), and Obo (plus)).

locations is 1–2 MJO phases, or 6–12 days. The minimum water level at these stations is in MJO phase 1, again delayed by 6–12 days from the minimum rainfall upstream and locally.

[49] Finally, the water level at the two stations furthest downriver (Manda, blue dash-dotted line with crosses; and Obo, blue dash-dotted line with pluses) is even further delayed, peaking in MJO phase 6. This is nearly in antiphase with rainfall inputs upstream; the delay is 1/4 to 3/8 MJO cycle.

6. Discussion

[50] Precipitation data at each of 15 stations on the Fly River system show a strong and a coherent MJO signal, one of the clearest reported from station data. Hence, the passage of the large-scale MJO envelope is clearly felt here at the local scale, which is more relevant for societal impacts. The station precipitation signal (both the mean and MJO cycle) is much stronger than in the state-of-the-art TRMM 3B42HQ precipitation data set, over the steep, high topography around the upper river catchment.

[51] There are known biases between the TRMM precipitation products and station rainfall [Cheema and Bastiaanssen, 2012]. Measuring precipitation using microwave remote sensing, as in the TRMM 3B42HQ product used here, has specific problems over orography. These are mainly due to changes in path length between the surface and satellite sensor, and the effects of rapidly changing slope angle and surface heterogeneity [Matzler and Standley, 2000].

[52] Several studies of TRMM precipitation over South and Central America have relevance to the results presented here. Over the Andes, the mapping of TRMM satellite data onto the 0.25° grid used in the 3B42 products was not able to retain the details over high and steep topography that was present in the original swath data, with a subsequent reduction in quality [Bookhagen and Strecker, 2008]. Rasmussen *et al.* [2013] found that the TRMM product underestimates precipitation from deep convection in South America generally; deep convection is a major component of precipitation over tropical mountainous regions such as New Guinea. Scheel *et al.* [2011] quantified the underestimation of rainfall by TRMM as a dry bias of 10 mm d⁻¹ for high (station) rainfall rates over 20 mm d⁻¹ in the Andes. This is consistent with the results found here in New Guinea.

[53] However, there are also examples of TRMM overestimating precipitation. Although TRMM underestimates rainfall in the wet season (October–March) in the Peruvian Andes, it overestimates it in the dry season (May–August) [Condom *et al.*, 2011]. Additionally, TRMM has been shown to overestimate precipitation over complex topography in certain conditions in Mexico [Montero-Martinez *et al.*, 2012]. These apparent systematic errors highlight the importance of ground truthing remotely sensed data and the pitfalls inherent in solely relying on such data.

[54] The peak rainfall within the MJO cycle occurs in MJO phase 4 (or occasionally phase 3) at all stations (Figure 5) and catchments (Figure 6). However, the exact timing of this peak (i.e., between phases 3 and 4) is not robust. For example, in the Lower Ok Tedi, two stations (Bige and Konkonda) show peak rainfall in phase 3, while

one station (Pump Stn Km 59) shows peak rainfall in phase 4 (Figure 5b). However, the median of the Lower Ok Tedi catchment event mean distribution has its peak in phase 4 (Figure 6c).

[55] Of more interest is that the peak (whether phase 3 or 4) should be so early in the MJO cycle. “Standard” MJO cycles using global satellite outgoing longwave radiation (OLR) have the peak convective envelope over and around New Guinea in phases 5–6 [e.g., Wheeler and Hendon, 2004], a quarter cycle later than observed in the station (and high-resolution TRMM) data. Two possible explanations have recently been put forward to explain this [Peatman *et al.*, 2014].

[56] The first is that the assumption that OLR is a good proxy for local rainfall in the tropics may not always be valid. Peatman *et al.* [2014] found a systematic lag in the MJO cycle between the peak in maximum rainfall over the islands of the maritime continent (including New Guinea) and the peak in minimum OLR, of about 1 MJO phase, i.e., 1/8 cycle. This could be due to the expansion of outflowing cirrus shields after the peak rainfall, leading to a later peak in minimum OLR (which measures cold cloud cover, not precipitation directly).

[57] The second explanation is related to the dynamics of the MJO itself. A “vanguard” of precipitation was found to jump ahead (eastward) of the main envelope over the islands of the maritime continent. This was due to a triggering of the diurnal cycle by solar radiation in the relatively clear skies ahead of the main MJO convective envelope. The low thermal inertia of the islands, compared to the surrounding ocean, and topographic moisture convergence allowed a strong diurnal cycle of precipitation to develop, which then interacted with the longer time scale MJO. The station rainfall results presented here add further evidence that the MJO behaves rather differently over the islands of the maritime continent compared to the surrounding seas.

[58] Aggregating up to the catchment scale, river level or height is an integrated measure of recent rainfall. The Fly River system shows a clear MJO signal in river level, the first to be observed. The river level peaks simultaneously with the MJO rainfall in the upper catchment but experiences an increasing lag further downstream. In the flood plains, the maximum river level lags the MJO precipitation by 3/8 cycle, i.e., into the *dry* phase of the MJO.

[59] The Ok Tedi mine, located in the upper catchment of the Fly River system, is of major economic importance to Papua New Guinea, accounting for over 30% of its export earnings. Precipitation and river level have a major impact on logistics, affecting both operations at the mine itself, and transportation of materials to and from the mine along the river. In particular, periods of low rainfall can lead to problems with the water supply at the mining town of Tabubil. Low river levels can severely disrupt and even shut down river transport. Because of the rapid response of the upper reaches of the river system to fluctuations in rainfall, a dry period of only two weeks, i.e., on MJO time scales, can make certain stretches of the river unnavigable. Low rainfall also impacts on subsistence gardening and fishing for local people in the surrounding areas.

[60] The large-scale features of the MJO can be skilfully forecast out to approximately 20 days lead time. Hence, local industrial operations, such as the Ok Tedi mine, could make

use of these forecasts operationally. Downscaling methods could be used in conjunction with the local station data to translate the large-scale MJO forecasts into locally relevant quantities along the Fly River. Given the large discrepancies between the station precipitation and the satellite-based TRMM precipitation in the vicinity of the mine, such downscaling is likely to be particularly important. Such forecasts would also be of use to local farming and fishing communities, though currently no suitable infrastructure exists to disseminate them.

[61] **Acknowledgments.** We thank Ok Tedi Mining Limited for providing the station data. The RMM index data were provided by the Centre for Australian Weather and Climate Research (www.cawcr.gov.au/staff/mwheeler/maproom). The TRMM 3B42HQ precipitation data were provided by NASA-Goddard (<http://trmm.gsfc.nasa.gov>). The GLOBE topography data were provided by NOAA-NGDC (<http://www.ngdc.noaa.gov/mgg/topo>). The research presented in this paper was carried out on the High Performance Computing Cluster supported by the Research Computing Service at the University of East Anglia. We thank three reviewers for their insightful comments that improved the analysis and the paper.

References

- Barlow, M., M. Wheeler, B. Lyon, and H. Cullen (2005), Modulation of daily precipitation over southwest Asia by the Madden–Julian Oscillation, *Mon. Weather Rev.*, **133**, 3579–3594.
- Bolton, B. R. (2009), *The Fly River, Papua New Guinea: Environmental Studies in an Impacted Tropical River System. Developments in Earth and Environmental Sciences*, vol. 9, Elsevier, Amsterdam.
- Bond, N. A., and G. A. Vecchi (2003), The influence of the Madden–Julian Oscillation on precipitation in Oregon and Washington, *weather forecast.*, **18**, 600–613.
- Bookhagen, B., and M. R. Strecker (2008), Orographic barriers, high-resolution TRMM rainfall, and relief variations along the eastern Andes, *Geophys. Res. Lett.*, **35**, L06403, doi:10.1029/2007GL032011.
- Cheema, M. J. M., and W. G. M. Bastiaanssen (2012), Local calibration of remotely sensed rainfall from the TRMM satellite for different periods and spatial scales in the Indus Basin, *Int. J. Remote Sens.*, **33**, 2603–2627.
- Condom, T., P. Rau, and J. C. Espinoza (2011), Correction of TRMM 3B43 monthly precipitation data over the mountainous areas of Peru during the period 1998–2007, *Hydrol. Process.*, **25**, 1924–1933.
- Donald, A., H. Meinke, B. Power, A. de H. N. Maia, M. C. Wheeler, N. White, R. C. Stone, and J. Ribber (2006), Near-global impact of the Madden–Julian Oscillation on rainfall, *Geophys. Res. Lett.*, **33**, L09704, doi:10.1029/2005GL025155.
- Hartmann, D. L., and M. L. Michelsen (1989), Intraseasonal periodicities in Indian rainfall, *J. Atmos. Sci.*, **46**, 2838–2862.
- Hastings, D. A., et al. (1999), The global land one-kilometer base elevation (GLOBE) digital elevation model, National Oceanic and Atmospheric Administration, National Geophysical Data Center, 325 Broadway, Boulder, CO 80303, USA.
- Huffman, G. J., R. F. Adler, D. T. Bolvin, G. J. Gu, E. J. Nelkin, K. P. Bowman, Y. Hoong, E. F. Stocker, and D. B. Wolff (2007), The TRMM multisatellite precipitation analysis (TMPA): Quasi-global, multiyear, combined-sensor precipitation estimates at fine scales, *J. Hydrometeorol.*, **8**, 38–55.
- Jones, C., L. M. V. Carvalho, R. W. Higgins, D. E. Waliser, and J. K. Schemm (2004), A statistical forecast model of tropical intraseasonal convective anomalies, *J. Clim.*, **17**, 2078–2095.
- Kanamori, H., T. Yasunari, and K. Kuraji (2013), Modulation of the diurnal cycle of rainfall associated with the MJO observed by a dense hourly rain gauge network at Sarawak, Borneo, *J. Clim.*, **26**, 4858–4875.
- Krishnamurthy, V., and J. Shukla (2000), Intraseasonal and interannual variability of rainfall over India, *J. Clim.*, **13**, 4366–4377.
- Love, B. S., A. J. Matthews, and G. J. Janacek (2008), Real-time extraction of the Madden–Julian Oscillation using empirical mode decomposition and statistical forecasting with a VARMA model, *J. Clim.*, **21**, 5318–5335.
- Love, B. S., and A. J. Matthews (2009), Real-time localised forecasting of the Madden–Julian Oscillation using neural network models, *Q. J. R. Meteorol. Soc.*, **135**, 1471–1483.
- Madden, R. A., and P. R. Julian (1971), Detection of a 40–50 day oscillation in the zonal wind in the tropical Pacific, *J. Atmos. Sci.*, **28**, 702–708.
- Madden, R. A., and P. R. Julian (1972), Description of global scale circulation cells in the tropics with a 40–50 day period, *J. Atmos. Sci.*, **29**, 1109–1123.
- Matthews, A. J., and H. Y. Y. Li (2005), Modulation of station rainfall over the western Pacific by the Madden–Julian Oscillation, *Geophys. Res. Lett.*, **32**, L14827, doi:10.1029/2005GL023595.
- Matzler, C., and A. Standley (2000), Relief effects for passive microwave remote sensing, *Int. J. Remote Sens.*, **21**, 2403–2412.
- Montero-Martinez, G., V. Zarraluqui-Such, and F. Garcia-Garcia (2012), Evaluation of 2B31 TRMM-product rain estimates for single precipitation events over a region with complex topographic features, *J. Geophys. Res.*, **117**, D02101, doi:10.1029/2011JD016280.
- Mutai, C. C., and N. M. Ward (2000), East African rainfall and the tropical circulation/convection on intraseasonal to interannual timescales, *J. Clim.*, **13**, 3915–3939.
- Nakazawa, T. (1988), Tropical super clusters within intraseasonal variations over the western Pacific, *J. Meteorol. Soc. Jpn.*, **66**, 823–839.
- Peatman, S. C., A. J. Matthews, and D. P. Stevens (2014), Propagation of the Madden–Julian Oscillation through the Maritime Continent and scale interaction with the diurnal cycle of precipitation, *Q. J. R. Meteorol. Soc.*, **140**, doi:10.1002/qj.2161.
- Rasmussen, K. L., S. L. Choi, M. D. Zuluaga, and R. A. Houze Jr. (2013), TRMM precipitation bias in extreme storms in South America, *Geophys. Res. Lett.*, **40**, 3457–3461, doi:10.1002/grl.50651.
- Salby, M. L., and H. H. Hendon (1994), Intraseasonal behavior of clouds, temperature, and motion in the tropics, *J. Atmos. Sci.*, **51**, 2207–2224.
- Scheel, M. L. M., M. Rohrer, C. H. Hugger, D. Santos Villar, E. Silvestre, and G. J. Huffman (2011), Evaluation of TRMM Multi-satellite Precipitation Analysis (TMPA) performance in the Central Andes region and its dependency on spatial and temporal resolution, *Hydrol. Earth Syst. Sci.*, **15**, 2649–2663.
- Sperber, K. R. (2003), Propagation and the vertical structure of the Madden–Julian oscillation, *Mon. Weather Rev.*, **131**, 3018–3037.
- Waliser, D. (2005), Predictability and forecasting, in *2005: Intraseasonal variability in the atmosphere-ocean climate system*, edited by W. K. M. Lau and D. E. Waliser, 389–424, Springer-Praxis, Berlin.
- Waliser, D., et al. (2009), MJO simulation diagnostics, *J. Clim.*, **22**, 3006–3030.
- Wheeler, M., and H. H. Hendon (2004), An all-season real-time multivariate MJO Index: Development of an index for monitoring and prediction, *Mon. Weather Rev.*, **132**, 1917–1932.
- Wilks, D. S. (2005), *Statistical Methods in the Atmospheric Sciences*, Academic Press, San Diego.
- Xie, P., and P. A. Arkin (1997), Global precipitation: A 17-year monthly analysis based on gauge observations, satellite estimates, and numerical model outputs, *Bull. Am. Meteorol. Soc.*, **78**, 2539–2558.
- Zhang, C. (2005), Madden–Julian Oscillation, *Rev. Geophys.*, **43**, RG2003, doi:10.1029/2004RG000158.
- Zhang, L., B. Wang, and Q. Zeng (2009), Impact of the Madden–Julian Oscillation on summer rainfall in southeast China, *J. Clim.*, **22**, 201–216.